Why asymmetric molecular coupling to electrodes cannot be at work in real molecular rectifiers

Ioan Bâldea *

Theoretical Chemistry, Heidelberg University, Im Neuenheimer Feld 229, D-69120 Heidelberg, Germany

(Received 10 March 2021; revised 22 April 2021; accepted 28 April 2021; published 7 May 2021)

Every now and then one hears in the molecular electronics community that asymmetric couplings ($\Gamma_s \neq \Gamma_t$) of the dominant level (molecular orbital) to electrodes (s and t) which typically have shapes different from each other may be responsible for current rectification observed in experiments. Using a general single level model going beyond the Lorentzian transmission limit, in this work we present a rigorous demonstration that this is not the case. In particular, we deduce an analytical for the bias (V)–driven shift of the level energy $\delta\varepsilon_0(V)$ showing that $\delta\varepsilon_0(V)/V$ scales as $\Gamma_t/W_t - \Gamma_s/W_s$, which is merely a tiny quantity because the electrode bandwidths $W_{s,t}$ are much larger than $\Gamma_{s,t}$. This result invalidates a previous, never deduced formula used in some previous publications that neither could be justified theoretically nor is supported by experiment. Toward the latter aim, we present new experimental evidence adding to that already inferred in earlier analyses.

DOI: 10.1103/PhysRevB.103.195408

I. INTRODUCTION

Current rectification ($\mathrm{RR} \equiv I(V)/|I(-V)| \neq 1$) using single-molecule devices, a topic pioneered by Aviram and Ratner [1], continues to represent a major topic of molecular electronics [2–18]. The present work is motivated by a confusion that persists regarding the physical origin of this phenomenon. It is generated by the fact that electrodes used to fabricate molecular junctions (planar substrate s and more or less sharp tip t) often have different shapes from each other. So, merely guided by naive intuition, one was often tempted to claim that the asymmetry in the measured current-voltage curves is just a manifestation of the electrodes' asymmetry. This issue has been addressed in a series of publications [19–24]. By postulating a Lorentzian transmission, an analytical formula [19,20,24–26] for the current I as a function of the applied bias V can easily be derived:

$$I = \frac{G_0}{e}\frac{2\Gamma_s\Gamma_t}{\Gamma_s+\Gamma_t}\left(\arctan\frac{2\varepsilon_0+eV}{\Gamma_s+\Gamma_t} - \arctan\frac{2\varepsilon_0-eV}{\Gamma_s+\Gamma_t}\right).$$

Here, e is the elementary charge, $G_0 = e^2/h = 77.48\ \mu\mathrm{S}$ is the conductance quantum, and $\varepsilon_0 = E_{\mathrm{MO}} - E_F$ the energy offset relative to the Fermi energy (E_F). Inspection of this formula immediately reveals that (in cases where ε_0 does not depend on V; see also Sec. IV D) the I-V curve is strictly symmetric irrespective of whether or not the MO couplings to electrodes Γ_s and Γ_t are equal. Rephrasing, $\Gamma_s \neq \Gamma_t$ does not result in current rectification:

$$\mathrm{RR}(V) \equiv -I(V)/I(-V) \neq 1.$$

The Lorentzian transmission is a phenomenological assumption that deserves quantum mechanical justification, at least based on a reasonable model Hamiltonian. Calculations using Keldysh's nonequilibrium formalism show that transmission is Lorentzian if the embedding self-energies $\Sigma_{s,t}$ quantifying the MO coupling to electrodes are assumed to be purely imaginary and energy independent:

$$\Sigma_{s,t} = -\frac{i}{2}\Gamma_{s,t}.$$

Still, even for a simple model Hamiltonian like that expressed by Eq. (1) below, the embedding self-energies are neither purely imaginary nor energy independent (see Sec. III). Do deviations of $\Sigma_{s,t}$ from the above form make it possible that merely unequal couplings ($\Gamma_s \neq \Gamma_t$) result in an observable current rectification ($\mathrm{RR} \neq 1$)?

Demonstrating that this is not the case is the general aim of this paper. Drawing attention to the incorrectness of a never demonstrated formula [namely, Eq. (18) below] yielding $\mathrm{RR} \neq 1$ for $\Gamma_s \neq \Gamma_t$ utilized in previous publications to quantitatively analyze current rectification in real molecular junctions is the most important specific aim of the present report.

II. THE SINGLE LEVEL MODEL

Let us consider the steady-state charge transport in a two-terminal setup consisting of a molecule (M) modeled as a single energy level ("molecular orbital"; MO) ε_0 linked to two electrodes, referred to as the "substrate" (label s) and "tip" (label t) subject to an external bias V. A general second quantized full Hamiltonian describing the charge transport mediated by a single energy level reads [26]

$$H = \underbrace{\sum_{l\leqslant -1}\left[\mu_s c_l^\dagger c_l - \left(t_s c_l^\dagger c_{l-1} + \mathrm{H.c.}\right)\right]}_{H_s} + \underbrace{\sum_{r\geqslant 1}\left[\mu_t c_r^\dagger c_r - \left(t_t c_r^\dagger c_{r+1} + \mathrm{H.c.}\right)\right]}_{H_t}$$

*ioan.baldea@pci.uni-heidelberg.de

$$\underbrace{-(\tau_s c_{-1}^\dagger c_0 + \text{H.c.})}_{H_{s,M}} + \underbrace{\varepsilon_0 c_0^\dagger c_0}_{H_M} \underbrace{-(\tau_t c_1^\dagger c + \text{H.c.})}_{H_{t,M}},$$
$$\varepsilon_0 \equiv \varepsilon_0(\ldots). \tag{1}$$

Above, the creation $c_{l,r}^\dagger$ and annihilation $c_{l,r}$ operators refer to single-electron states in the substrate's and tip's conduction band of widths $W_{s,t} = 4|t_x|$, respectively. The subscript 0 refers to the single molecular level considered, and $\tau_{s,t}$ are effective (average) exchange integrals quantifying the MO-electrode charge transfers. For the sake of simplicity, electron spin is not included explicitly but its contribution (a multiplicative factor of 2) is accounted for whenever physically relevant [e.g., Eq. (11)]. The strong on-site Coulomb repulsion [25,27] implicitly assumed in Eq. (11) precludes level double occupancy and leaves Coulomb blockade and the Kondo effect beyond the present consideration. [Please note that typical ionization energies ($IP \sim 10$ eV) in real molecules are very large, much larger than (HO)MO offsets relative to the electrode's Fermi energy $|\varepsilon_0| \lesssim 1$ eV.]

In the presently considered zero-temperature case, single-particle electron states in electrodes are filled up to energies below the electrodes' (electro)chemical potential μ_x ($x = s, t$), whose imbalance

$$\mu_{s,t} = E_F \pm eV/2, \quad \mu_s - \mu_t = eV \tag{2}$$

caused by an applied bias V gives rise to an electric current through the junction on which we focus next. Note that by virtue of Eq. (2) $V > 0$ means a positive-t (tip) electrode, an aspect of practical relevance when discussing the direction of rectification in specific real junctions.

Noteworthily, Eq. (11) by no means rules out a V dependence of ε_0. This may arise when the level (MO) center of charge is located asymmetrically with respect to the electrodes ("lever" [19] or "potentiometer" [23,28] rule) or due to the intramolecular Stark effect, a point to which we return at the end of Sec. IV D. It is what we mean by the ellipsis ("...") in the last line of Eq. (1).

Provided that the Hamiltonian is the same for "forward" and "backward" current flow, there cannot be rectification. This is a completely general result, independent of details of models; an example is what was called the zero-current theorem in studies on generic tight-binding models [29,30]. The point in the specific case presently considered is that, albeit oversimplified, provided that $t_s \neq t_t$ and $\tau_s \neq \tau_t$, the model Hamiltonian, Eq. (1), does allow forward and backward currents to be different $I(-V) \neq -I(V)$ even if ε_0 does not depend on V. So, in principle Eq. (1) is compatible with $\text{RR}(V) \neq 1$. This is substantiated by Eq. (10) deduced below: an exact result, demonstrating that current rectification can occur. The important problem is, however, whether this broken "left-right" symmetry ($c_l \rightleftharpoons c_r$, $c_l^\dagger \rightleftharpoons c_r^\dagger$, $V \rightleftharpoons -V$) of Eq. (1) can be the source of an *observable* current rectification.

III. GENERAL RESULTS

Within the Keldysh formalism [31], the key quantity needed to express the current I (see Eq. (11) below [32–35]) through a molecular junction is the retarded Green's function G^R of the "embedded" molecule. It is related to the retarded Green's function of the isolated molecule

$$G_0^R(\varepsilon) = 1/(\varepsilon - \varepsilon_0 + i0^+)$$

via Dyson's equation

$$[G^R(\varepsilon)]^{-1} = \left[G_0^R(\varepsilon)\right]^{-1} - \Sigma_s(\varepsilon) - \Sigma_t(\varepsilon). \tag{3}$$

The embedding self-energies $\Sigma_{s,t}$ have the form [34,36,37]

$$\Sigma_x(\varepsilon) \equiv \Delta_x(\varepsilon) - \frac{i}{2}\Gamma_x(\varepsilon) = |\tau_x|^2 g_x^R(\varepsilon) \tag{4}$$

and account for the MO coupling to electrodes via the average exchange integrals of the MO-electrode couplings τ_x [33,36]. The (surface) retarded Green's functions of the semi-infinite electrodes can be expressed in closed analytical forms [37–40],

$$g_x^R(\varepsilon) = 8\frac{\varepsilon - \mu_x}{W_x^2} - i\frac{4}{W_x}\sqrt{1 - 4\left(\frac{\varepsilon - \mu_x}{W_x}\right)^2}. \tag{5}$$

Below, we confine ourselves to typical situations where applied biases yield an imbalance of the electrodes' electrochemical potential sufficiently smaller than the electrodes' bandwidth $e|V| < W_x/2$, ensuring thereby that the square roots entering the right-hand side of Eqs. (5) and (8a) are real numbers. Otherwise, the electrodes' finite band may give rise to negative differential resistance effects, as discussed elsewhere [26].

The electrode's density of states (DOS) $\rho_x(\varepsilon)$ can be written as

$$\rho_x(\varepsilon) \equiv -\frac{1}{\pi}\,\text{Im}\, g_x^R(\varepsilon) = \frac{4}{\pi}\frac{1}{W_x}\sqrt{1 - 4\left(\frac{\varepsilon - \mu_x}{W_x}\right)^2} \tag{6}$$

and has at the Fermi energy the value

$$\rho_x \equiv \rho_x(\varepsilon)|_{\varepsilon=\mu_x} = \frac{4}{\pi}\frac{1}{W_x} = \frac{1.2733}{W_x}, \tag{7}$$

which is basically the inverse of the electrode's conduction bandwidth.

Based on the aforementioned, analytical forms for Δ_x and Γ_x can be deduced [26]:

$$\Gamma_x(\varepsilon) = \Gamma_x\sqrt{1 - 4\left(\frac{\varepsilon - \mu_x}{W_x}\right)^2}, \quad \Gamma_x \equiv 8\frac{|\tau_x|^2}{W_x}; \tag{8a}$$

$$\Delta_x(\varepsilon) = \frac{\Gamma_x}{W_x}(\varepsilon - \mu_x) = \frac{\pi}{4}\Gamma_x\rho_x(\varepsilon - \mu_x). \tag{8b}$$

One should note here that the expression of Γ_x in terms of ρ_x deduced from Eqs. (7) and (8a),

$$\Gamma_x = 2\pi\rho_x|\tau_x|^2,$$

is not restricted to the case of the semielliptic DOS in Eq. (6) [2,33,41,42]. Including MO-electrode interactions beyond the choice for $H_{x,M}$ adopted in Eq. (1) is possible [2,43] but is not attempted here because the pertaining corrections were shown [44] not to substantially alter the conclusions based on Eq. (6).

The closed form of the retarded Green's function describing the junction under applied bias ($V \neq 0$) can now be obtained by inserting Eqs. (8a) and (8b) into the Dyson equation, (3):

$$G^R(\varepsilon) = \frac{1}{1-\frac{\Gamma_s}{W_s}-\frac{\Gamma_t}{W_t}} \frac{1}{\varepsilon - \tilde{\varepsilon}_0(V) + \frac{i}{2}[\tilde{\Gamma}_s(\varepsilon)+\tilde{\Gamma}_t(\varepsilon)]}, \tag{9a}$$

$$\tilde{\Gamma}_s(\varepsilon) \equiv \Gamma_s \frac{\sqrt{1-4\left(\frac{\varepsilon - eV/2}{W_s}\right)^2}}{1-\frac{\Gamma_s}{W_s}-\frac{\Gamma_t}{W_t}}, \tag{9b}$$

$$\tilde{\Gamma}_t(\varepsilon) \equiv \Gamma_t \frac{\sqrt{1-4\left(\frac{\varepsilon + eV/2}{W_s}\right)^2}}{1-\frac{\Gamma_s}{W_s}-\frac{\Gamma_t}{W_t}}. \tag{9c}$$

The retarded Green's function has a "pole" (more precisely, this is the position where the real part of $[G^R(\varepsilon)]^{-1}$ vanishes) at

$$\tilde{\varepsilon}_0(V) = \tilde{\varepsilon}_0 + \delta\tilde{\varepsilon}_0(V) = \tilde{\varepsilon}_0 + \gamma eV, \tag{10a}$$

$$\tilde{\varepsilon}_0 = \frac{\varepsilon_0}{1-\frac{\Gamma_s}{W_s}-\frac{\Gamma_t}{W_t}} = \varepsilon_0\left(1+\frac{\Gamma_s}{W_s}+\frac{\Gamma_t}{W_t}\right) + O\left(\frac{\Gamma_{s,t}}{W_{s,t}}\right)^2, \tag{10b}$$

$$\gamma = \frac{1}{2}\frac{\frac{\Gamma_t}{W_t}-\frac{\Gamma_s}{W_s}}{1-\frac{\Gamma_s}{W_s}-\frac{\Gamma_t}{W_t}} = \frac{1}{2}\left(\frac{\Gamma_t}{W_t}-\frac{\Gamma_s}{W_s}\right) + O\left(\frac{\Gamma_{s,t}}{W_{s,t}}\right)^2, \tag{10c}$$

which defines the MO energy $\tilde{\varepsilon}_0(V)$ of the embedded molecule in a current-carrying state. Note that Eq. (10) includes both the MO energy renormalization due to the couplings to electrodes ($\Gamma_{s,t} \neq 0$) of the molecule embedded in the unbiased ($V \equiv 0$) junction ($\varepsilon_0 \to \tilde{\varepsilon}_0 \neq \varepsilon_0$) and the bias-driven MO energy renormalization [$V \neq 0 \to \delta\tilde{\varepsilon}_0(V) = \gamma eV \neq 0$].

Inserting the above expressions into the general formula [32,34,36]

$$I = \frac{2e}{h}\int_{\mu_s}^{\mu_t} d\,\varepsilon \Gamma_s(\varepsilon)\Gamma_t(\varepsilon)|G^R(\varepsilon)|^2, \tag{11}$$

we are led to the general expression of the current determined by a single transport channel ("single level model") at zero temperature,

$$I = \frac{2e}{h}\int_{-eV/2}^{eV/2} \frac{\tilde{\Gamma}_s(\varepsilon)\tilde{\Gamma}_t(\varepsilon)}{[\varepsilon - \tilde{\varepsilon}_0(V)]^2 + \frac{[\tilde{\Gamma}_s(\varepsilon)+\tilde{\Gamma}_t(\varepsilon)]^2}{4}} d\,\varepsilon. \tag{12}$$

Along with Eq. (12), the expression of the local density of states,

$$\mathrm{LDOS}(\varepsilon) \equiv -\frac{1}{\pi}\mathrm{Im}G^R(\varepsilon) = \frac{1}{\pi}\frac{1}{1-\frac{\Gamma_s}{W_s}-\frac{\Gamma_t}{W_t}} \frac{\frac{1}{2}[\tilde{\Gamma}_s(\varepsilon)+\tilde{\Gamma}_t(\varepsilon)]}{[\varepsilon - \tilde{\varepsilon}_0(V)]^2 + \frac{1}{4}[\tilde{\Gamma}_s(\varepsilon)+\tilde{\Gamma}_t(\varepsilon)]^2}, \tag{13}$$

better allows us to emphasize the twofold role played by $\tilde{\Gamma}_{s,t}(\varepsilon)$: renormalized MO couplings to electrodes (entering as multiplicative factors in Eq. (12)) and renormalized partial level broadenings [cf. Eq. (13)].

Equation (10) allows us to disentangle the impact of the MO couplings' renormalization [$\Gamma_{s,t} \leftarrow \tilde{\Gamma}_{s,t}(\varepsilon)$, $I_\Gamma \leftarrow I$],

$$I_\Gamma = \frac{2e}{h}\int_{-eV/2}^{eV/2} \frac{\tilde{\Gamma}_s(\varepsilon)\tilde{\Gamma}_t(\varepsilon)}{(\varepsilon - \varepsilon_0)^2 + \frac{[\tilde{\Gamma}_s(\varepsilon)+\tilde{\Gamma}_t(\varepsilon)]^2}{4}} d\,\varepsilon, \tag{14}$$

from the impact of the MO energy renormalization [$\varepsilon_0 \leftarrow \tilde{\varepsilon}_0(V)$, $I_\varepsilon \leftarrow I$],

$$I_\varepsilon = \frac{2e}{h}\frac{1}{\left(1-\frac{\Gamma_s}{W_s}-\frac{\Gamma_t}{W_t}\right)^2}\int_{-eV/2}^{eV/2} \frac{\Gamma_s\Gamma_t}{[\varepsilon - \tilde{\varepsilon}_0(V)]^2 + \frac{(\Gamma_s+\Gamma_t)^2}{4}} d\,\varepsilon.$$

The latter can be integrated out in closed form and reads

$$I_\varepsilon = \frac{G_0/e}{\left(1-\frac{\Gamma_s}{W_s}-\frac{\Gamma_t}{W_t}\right)^2}\frac{2\Gamma_s\Gamma_t}{\Gamma_s+\Gamma_t} \times\left[\arctan\frac{2\tilde{\varepsilon}_0(V)+eV}{\Gamma_s+\Gamma_t} - \arctan\frac{2\tilde{\varepsilon}_0(V)-eV}{\Gamma_s+\Gamma_t}\right], \tag{15}$$

where $\tilde{\varepsilon}_0(V)$ is given by Eq. (10). If the charge transport occurs sufficiently far away from resonance (which is the usual case [45,46]), i.e.,

$$[2|\tilde{\varepsilon}_0(V) - |eV|]/[\Gamma_s+\Gamma_t] \gg 1,$$

Eq. (15) is amenable in the simpler form [47]

$$I_\varepsilon \simeq I_{\text{off-res}} = \frac{\Gamma_s\Gamma_t}{\left(1-\frac{\Gamma_s}{W_s}-\frac{\Gamma_t}{W_t}\right)^2}\frac{G_0V}{\tilde{\varepsilon}_0^2(V) - (eV/2)^2}. \tag{16}$$

In the wide-band limit ($W_{s,t} \to \infty$), $\Gamma_{s,t}(\varepsilon) \to \Gamma_{s,t}$, $\tilde{\varepsilon}_0(V) \to \varepsilon_0$, and Eqs. (15) and (16) reduce to Eqs. (3) and (4) in Ref. [47].

As a hybrid approximation, one can also consider couplings' renormalization only in the numerator of the integrand entering the right-hand side of Eq. (12):

$$I_{\varepsilon(\Gamma)} = \frac{2e}{h}\int_{-eV/2}^{eV/2} \frac{\tilde{\Gamma}_s(\varepsilon)\tilde{\Gamma}_t(\varepsilon)}{[\varepsilon - \tilde{\varepsilon}_0(V)]^2 + \frac{(\Gamma_s+\Gamma_t)^2}{4}} d\,\varepsilon. \tag{17}$$

IV. DISCUSSION

Inspection of Eq. (12) reveals that, *in principle*, rectification $I(-V) \neq -I(V)$ could arise in junctions whose electrodes have different properties ($\Gamma_s \neq \Gamma_t$, $W_s \neq W_t$). Based on it, we next examine how *effective* the impact of electrodes' asymmetry on current rectification in real junctions is.

A. General considerations

According to Eq. (12), values of rectification RR $\neq 1$ (i) could be the result of a polarity-dependent bias-driven MO shift due to the couplings' asymmetry, $\delta\tilde{\varepsilon}_0(-V) \neq \delta\tilde{\varepsilon}_0(V)$, and/or (ii) could be because the expressions in parentheses under the square root entering Eqs. (9b) and (9c) pertaining to

the substrate and tip electrodes are significantly different from each other and at least one of them is significantly different from 0.

Regarding (i): Equation (10c) yields

$$\gamma = \frac{1}{2}\left(\frac{\Gamma_t}{W_t} - \frac{\Gamma_s}{W_s}\right) + O\left(\frac{\Gamma_{s,t}}{W_{s,t}}\right)^2 \approx \frac{1}{2}\left(\frac{\Gamma_t}{W_t} - \frac{\Gamma_s}{W_s}\right),$$

which should make it clear that a bias-driven MO energy shift can safely be ruled out. Indeed, even if the effective value $W = 35.8$ eV deduced for gold from the DOS $\rho = 0.035\ \mathrm{eV}^{-1}$ [44,48] via Eq. (7) might be somewhat overestimated, it still substantiates the conclusion that W is much larger than the MO-electrode couplings Γ; values of Γ estimated for real junctions are at most $\sim 10^{-1}$ eV, typically a few meV [45,46,49,50].

Although not directly related to rectification, we note in passing that, for the same reason, a substantial change in MO energy offset *merely* due to molecule embedding [i.e., $\tilde{\varepsilon}_0 \neq \varepsilon_0$, cf. Eq. (10b)] cannot occur,

$$\tilde{\varepsilon}_0 = \varepsilon_0\left(1 + \frac{\Gamma_s}{W_s} + \frac{\Gamma_t}{W_t}\right) + O\left(\frac{\Gamma_{s,t}}{W_{s,t}}\right)^2$$
$$\approx \varepsilon_0\left(1 + \frac{\Gamma_s}{W_s} + \frac{\Gamma_t}{W_t}\right) \approx \varepsilon_0.$$

Regarding (ii): Given the fact that the integration variable entering the right-hand side of Eq. (12) varies in the range $|\varepsilon| < e|V|/2$, the maximum values of the expressions in parentheses under the square root are $(V/W_{s,t})^2$. This again shows that, at the highest bias values, $V \sim 1$ V, applied in real experiments, differences between currents at positive and negative polarities can hardly exceed $\sim 0.1\%$.

B. Specific examples: Two benchmark cases

Having said this in general, let us focus on two benchmark junctions fabricated with octanethiol (C8T) and 1,1′, 4′, 1″-terphenyl-4-thiol (OPT3 in Ref. [46]) molecules. The parameters $\varepsilon_0 \equiv -\varepsilon_h$, Γ_s, and Γ_t that make this analysis possible are available or can be estimated thanks to recent extensive investigations on these monothiolates [45,46] as well as on their dithiolate (C8DT [46] and OPD3 [49]) counterparts. Data for dithiols (d) are also needed because, while providing values of the (geometric) average $\Gamma = \sqrt{\Gamma_s \Gamma_t}$ [47], transport data for a given molecular species do not allow the separate determination of the two individual components Γ_s and Γ_t for the presently considered monothiols (m).

In view of the fact that not only self-assembled monolayers (SAMs) deposited on gold but also junctions fabricated with those dithiols are characterized by extremely small statistical variations in their transport properties [51], it is legitimate to assume that $\Gamma_s^d \approx \Gamma_t^d \approx \Gamma^d$; dithiolate species form stable covalent bonds responsible for chemisorption both at the substrate and at the tip. In addition, one can assume that $\Gamma_s^m \approx \Gamma_s^d \approx \Gamma^d$; both monothiols and dithiols are linked to the substrate by thiol groups. Doing so, based on $\Gamma^{C8DT} = 14.88$ meV [46] and $\Gamma^{C8T} = 2.45$ meV [46], we get $\Gamma_s^{C8T} = 14.88$ meV and $\Gamma_t^{C8T} = (\Gamma^{C8T})^2/\Gamma_s^{C8T} = 0.40$ meV. Similarly, using $\Gamma^{\mathrm{OPD3}} = 18.34$ meV [45] and $\Gamma^{\mathrm{OPT3}} = 4.52$ meV [45] we estimate $\Gamma_s^{\mathrm{OPT3}} = 18.34$ meV and $\Gamma_t^{\mathrm{OPT3}} = (\Gamma^{\mathrm{OPT3}})^2/\Gamma_s^{\mathrm{OPT3}} = 1.11$ meV.

Figures 1 and 2 depict the dependence on bias of the current rectification obtained by using the HOMO offsets derived from recent transport measurements ($\varepsilon_0^{C8T} \equiv -\varepsilon_h^{C8T} = -1.01$ eV [46] and $\varepsilon_0^{\mathrm{OPT3}} \equiv -\varepsilon_h^{\mathrm{OPT3}} = -0.66$ eV [45]) along with the aforementioned values of $\Gamma_{s,t}$. As shown by the blue curves in Figs. 1(b) and 2(b), the impact of $\Gamma_{s,t}$ renormalization brought about by applied bias is completely negligible. The "largest" contribution to rectification comes from the renormalization of the HOMO energy, which is accounted for by Eq. (15) and depicted by the magenta curves. In off-resonant situations and biases of experimental interest this effect is very accurately described by the simpler Eq. (16), which represents the generalization beyond the wide-band approximation of a result (Eq. (4) in Ref. [47]) deduced earlier in the limit $W_x \to \infty$.

To sum up, Figs. 1 and 2 clearly reveal that, when fully accounted for, renormalization effects due to MO couplings to the electrodes of C8T and OPT3 junctions are unable to make RR significantly different from unity and are by no means responsible for the values observed in experiments ($\mathrm{RR}_{OPT3} \simeq 2.5$ at $V = 1.2$ V and $\mathrm{RR}_{C8T} \simeq 0.7$ at $V = 1.5$ V) [28,45,46]. To make this point clearer, in addition to calculations based on parameter values deduced from experimental data (see above), we also performed companion simulations to artificially enhance the impact of the aforementioned renormalization, ruling out that possible parameters' inaccuracy may vitiate the conclusions presented below. For example:

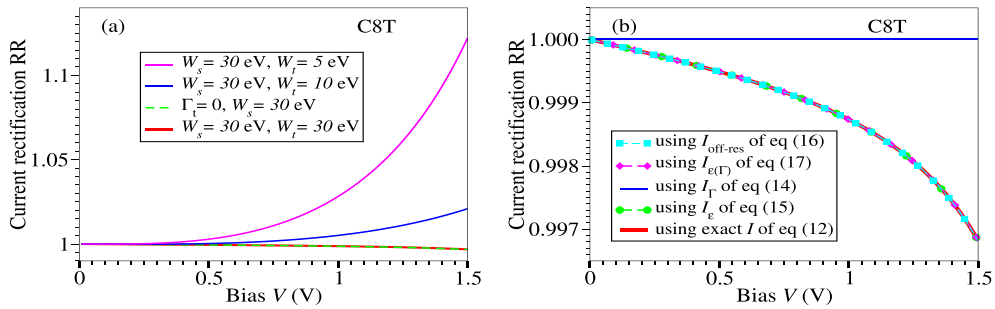

FIG. 1. Current rectification RR calculated in the experimentally relevant bias range using parameters (a) estimated for C8T junctions [46] and (b) modified to overestimate the RR values. See Sec. IV B for details.

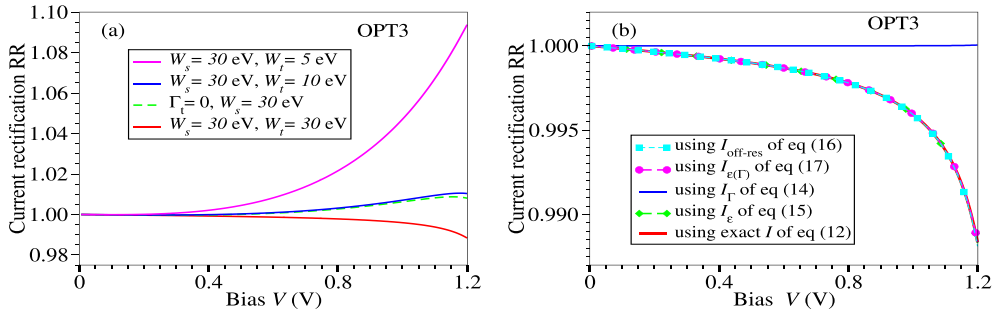

FIG. 2. Current rectification RR calculated in the experimentally relevant bias range using parameters (a) estimated for OPT3 junctions [45] and (b) modified to overestimate the RR values. See Sec. IV B for details.

(i) We considered the case of extreme asymmetric couplings to electrodes ($\Gamma_t \to 0$). Calculations for this case [green curves in Figs. 1(a) and 2(a)] yield values of RR that cannot be practically distinguished from unity.

(ii) We performed simulations by using electrode bandwidths W_t substantially smaller than that previously estimated ($W_{Au} = 35.8$ eV [44,48]; see above). Letting alone the comparative purpose, the rationale for this choice might be that, unlike practically infinite substrates, more or less sharp tips may have DOS values [$\rho_x \approx 1/W_x$; cf. Eq. (6)] different from the value for infinite metal. Note again that by choosing a smaller W_t value, renormalization effects are (artificially) overestimated: W's enter the denominators of relevant formulas, e.g., Eq. (12). Results of these calculations are depicted by the blue and magenta curves in Figs. 1(a) and 2(a). The emerging conclusion is the same; although overestimated, this rectification RR $= 1 \pm 0.0\ldots$ substantially departs from that deduced from experiments and lacks any practical relevance.

C. Interrogating possible charge accumulation effects at contacts

The exact results reported above in this section have substantiated what the title states: The $\Gamma_{s,t}$ couplings' asymmetry does not have a quantitatively relevant impact on current rectification. But, after all, this conclusion is based on a highly simplified model. So, one may wonder whether the unequal charge transfer rates $\Gamma_s \neq \Gamma_t$ may still significantly enhance the completely negligible current asymmetry $I(+V) \neq |I(-V)|$ via physical effects escaping Eq. (1). Being driven by unequal $\Gamma_s \neq \Gamma_t$, the effectt discussed next belongs in this category.

Fabrication of a molecular junction necessarily implies a certain (possibly asymmetric) charge exchange between the embedded molecule and the electrodes which cannot be ignored even within a single-electron description like that underlying Eq. (1); the level's energy *is* renormalized [cf. Eq. (10)] but this is a wispy effect. If the extra electronic charge accumulated at the "interface positions" [which are denoted by $l = -1$ and $r = 1$ in Eq. (1)] were significantly dependent on the bias polarity, this would be a relevant point deserving consideration in the present context of rectification. If this were the case and the MO occupancy significantly changed upon bias polarity reversal, one would have to consider the associated electrostatic interactions (preferably treated within a many-body picture, since this turned out to be feasible [20]) as a potential source of rectification.

With this in mind, we computed the bias-dependent MO occupancy $n_0 = \langle c_0^\dagger c_0 \rangle$ as well as the occupancies $n_s \equiv \langle c_l^\dagger c_l \rangle|_{l=-1}$ and $n_t \equiv \langle c_r^\dagger c_r \rangle|_{r=1}$ at the contacts. This is an easy task because, in the absence of electron correlations, the nonequilibrium Keldysh lesser Green's functions ($\mathbf{G}^<$) needed can be straightforwardly expressed in terms of the retarded Green's functions. Being a rather marginal issue in this paper we skip the technical details; all relevant information can be found in Ref. [52]. The results of these calculations using the model parameters deduced in Sec. IV B for C8T are collected in Fig. 3. Within the model considered, the differences $n_0 \neq 1$ and $n_{s,t} \neq 1/2$ shown in Fig. 3 reflect the combined effect of coupling to electrodes ($\Gamma_{s,t} \neq 0$) and applied bias ($V \neq 0$). The highly localized C8T's HOMO concentrated in the immediate vicinity of the substrate (e.g., Fig. 6 in Ref. [23]) makes the impact on n_s "stronger" than that on n_t; compare Figs. 3(b) and 3(c). Still, most importantly in the present context, for all biases of experimental relevance, V has an altogether negligible impact on all electron occupancies. This rules out any notable contribution to current rectification.

Above, we have intentionally restricted ourselves to the case of C8T. The much less spatially asymmetric OPT3's HOMO delocalized over the entire molecule (e.g., Fig. S7 in Ref. [45]) makes the difference $n_s \neq n_t$ in this molecular species even substantially smaller than for C8T.

D. Additional remarks

We do not want to end this work without commenting on earlier literature attempts to describe current rectification by postulating a bias-driven energy shift of the single dominant transport channel depending on the coupling to electrodes $\Gamma_{s,t}$ [53–56] as

$$V_s \equiv -\frac{V}{2} \leqslant V \leqslant V_t \equiv \frac{V}{2},$$

$$\varepsilon_0|_{V=0} \xrightarrow{V\neq 0} \varepsilon_0(V) = \varepsilon_0 + \overline{\gamma}\, eV, \tag{18a}$$

$$\overline{\gamma} = \frac{1}{2}\frac{\Gamma_s - \Gamma_t}{\Gamma_s + \Gamma_t} = \frac{1}{2}(1-\delta), \quad \delta \equiv \frac{2\Gamma_t}{\Gamma_s + \Gamma_t} \tag{18b}$$

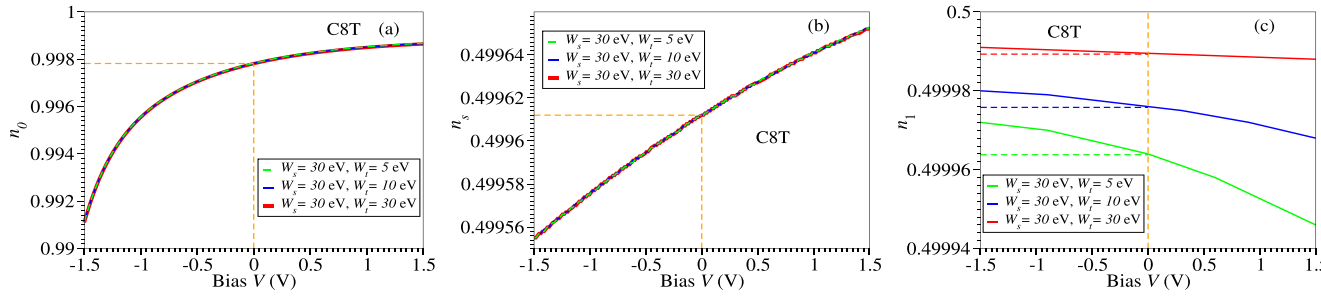

FIG. 3. The bias dependence of the occupancies n_j of (a) the HOMO and the adjacent sites in (b) substrate and (c) tip electrodes computed using parameters estimated for C8T junctions and modified to overestimate the RR values. See Fig. 1 and Sec. IV B for details.

or equivalently

$$V_s' \equiv 0 \leqslant V \leqslant V_t' \equiv V, \quad \varepsilon_0'|_{V=0} \xrightarrow{V\neq 0} \varepsilon_0'(V) = \varepsilon_0 + \eta\, eV, \tag{19a}$$

$$\eta = \frac{\Gamma_s}{\Gamma_s + \Gamma_t} = \frac{1}{2} + \overline{\gamma}. \tag{19b}$$

Note that due to the different choice of the electric potential origin, $\varepsilon_0'(V) = \varepsilon_0(V) + eV/2$ and $\eta = 1/2 + \overline{\gamma}$. $\mu_s - \mu_t = eV$ holds in both cases, implying, e.g., a positive bias on t (the tip) for $V > 0$.

Importantly for checking its validity against experimental data, Eq. (18) predicts that the *direction* of the MO bias-driven shift (upwards or downwards) is merely dependent on the sign of the couplings' difference $\Gamma_s - \Gamma_t$,

$$\delta\varepsilon_0(V) \equiv \varepsilon_0(V) - \varepsilon_0(V)|_{V=0} = \overline{\gamma} eV = \frac{1}{2}\frac{\Gamma_s - \Gamma_t}{\Gamma_s + \Gamma_t} eV \propto \mathrm{sgn}(\Gamma_s - \Gamma_t)\,\mathrm{sgn}V,$$

which translates into a current rectification (RR) direction (i.e., RR > 1 or RR < 1) merely dependent on the sign of $\Gamma_s - \Gamma_t$ expressed as

$$\mathrm{RR}_{\mathrm{HOMO}}(V>0) \equiv -\frac{I(V)}{I(-V)} \begin{cases} >1 & \text{for} \quad \overline{\gamma} > 0 \Rightarrow \Gamma_s > \Gamma_t \\ <1 & \text{for} \quad \overline{\gamma} > 0 \Rightarrow \Gamma_s < \Gamma_t \end{cases} \quad \text{for HOMO-mediated conduction} \quad (\varepsilon_0 < 0)$$

and

$$\mathrm{RR}_{\mathrm{LUMO}}(V>0) \equiv -\frac{I(V)}{I(-V)} \begin{cases} <1 & \text{for} \quad \overline{\gamma} > 0 \Rightarrow \Gamma_s > \Gamma_t \\ >1 & \text{for} \quad \overline{\gamma} < 0 \Rightarrow \Gamma_s < \Gamma_t \end{cases} \quad \text{for LUMO-mediated conduction} \quad (\varepsilon_0 > 0).$$

Although neither deduced theoretically nor validated experimentally, the expression for $\overline{\gamma}$ of Eq. (18b)—or equivalently quantity $\eta = 1/2 + \overline{\gamma} = \Gamma_s/(\Gamma_s + \Gamma_t)$ mentioned above—was utilized in previous publications, e.g., for textbook, illustrative purposes [53] or (sometimes [54]) aware of the fact that a $\Gamma_{s,t}$ asymmetry similar to the asymmetry in the voltage drop is merely an assumption made for the sake of simplicity. The minor difference between $\eta = \Gamma_s/(\Gamma_s + \Gamma_t)$ [53,54] and $\overline{\gamma}$ in our Eq. (18b) is due to the different choice of the potential origin; the former chose $V_s = 0$, $V_t = V$, while we used $V_s = -V/2$, $V_t = V/2$ [cf. Eq. (2)].

As shown, the *never* deduced Eq. (18b) has no resemblance to our Eq. (10c), a formula *deduced* here within a general single level model. Although of little practical importance because we have shown above that the bias-driven MO shift due to $V \neq 0$ and coupling to electrodes expressed by Eq. (10) is altogether negligible, it can still be remarked that even the shift direction of the never deduced Eq. (18) may be problematic: $\overline{\gamma} \propto \mathrm{sgn}(\Gamma_s - \Gamma_t)$ [cf. Eq. (18b)] as opposed to $\gamma \propto \mathrm{sgn}(\Gamma_t - \Gamma_s)$ [cf. Eq. (10c)] for $W_s = W_t$).

By and large, one should conclude that Eq. (18) has no theoretical support. This analytical demonstration adds additional evidence to the fact emphasized earlier that the I-V asymmetry predicted by Eq. (18b) is at odds with various experimental data collected under various platforms (see Refs. [23,57], and citations therein).

Besides the examples presented earlier [57,58], let us demonstrate that the transport data for the presently considered C8T and OPT3 junctions also invalidate Eq. (18). Indeed, inserting the values of Γ_s and Γ_t from Sec. IV B into Eq. (18b) we get via $\overline{\gamma}_{C8T} = 0.47$ for C8T and $\overline{\gamma}_{OPT3} = 0.44$ for OPT3. With $\varepsilon_0(V)$ in Eq. (18) this translates into $\mathrm{RR}|_{V=1.5\,\mathrm{V}} = 652(\gg 1)$ for C8T and $\mathrm{RR}|_{V=1.2\,\mathrm{V}} = 282(\gg 1)$ for OPT3. These values are not only quantitatively but also qualitatively different from the experimental values: $\mathrm{RR}^{exp}|_{V=1.5\,\mathrm{V}} \simeq 0.7 < 1$ [46] and $\mathrm{RR}^{exp}|_{V=1.2\,\mathrm{V}} \simeq 2.5 > 1$ [45]. For a more complete overview of the unsuitability of Eq. (18), all present and earlier values mentioned above are compiled in Table I and depicted graphically in Fig. 4.

Put conversely, let us now assume that Eq. (18b) was correct (i.e., $\overline{\gamma} = \gamma_{\mathrm{real}}$) and applied to the OPT3 junctions considered above. (Remember that this cannot be done for C8T junctions wherein $\gamma_{\mathrm{real}} \equiv \gamma_{\mathrm{exp}} = -0.03$ [46] would imply $\Gamma_t > \Gamma_s$ and hence, completely unrealistically, a charge transfer rate Γ_s between the substrate and the HOMO located in its close vicinity smaller than the HOMO-tip charge transfer

TABLE I. Values of $\gamma_{\text{real}} \to \gamma_{\text{exp}}$, δ, and $\overline{\gamma}$ for several molecular junctions investigated experimentally.

γ_{real}	δ	$\overline{\gamma}$	System
0.056[a]	0.115[f]	0.443[g]	CP-AFM, OPT3 [46]
−0.035[b]	0.053[f]	0.474[g]	CP-AFM, C8T [45]
0.060[c],[d]	1.1e-4[c]	0.500[g]	EC-STM (variable bias mode), azurin [59]
−0.305[d,e]	0.015[e]	0.492[g]	EC-STM (variable bias mode), viologen [60]
−0.270[d,e]	0.015[e]	0.492[g]	EC-STM (constant bias mode), viologen [60]

[a]From Ref. [46].
[b]From Ref. [45].
[c]From Ref. [58].
[d]Note that γ in Refs. [58,57] corresponds to $\gamma_{\text{real}} = 1/2 - \gamma$.
[e]From Ref. [57].
[f]From this work.
[g]From this work via Eq. (18b).

rate Γ_t across the long alkyl backbone.) With the value $\gamma_{\text{real}} \equiv \gamma_{\text{exp}} = 0.055$ extracted from OPT3 *I*-*V* data [45], we get $\Gamma_s^{\text{OPT3}} = \Gamma^{\text{OPT3}}\sqrt{(1+2\overline{\gamma})/(1-2\overline{\gamma})} = 5.05$ meV. Being substantially smaller than $\Gamma_s^{\text{OPD3}} = 18.34$ meV (cf. Sec. IV B), this value, $\Gamma_s^{\text{OPT3}} = 5.05$ meV, is unphysical; located at the center of the symmetrical OPD3 molecule, OPD3 HOMO's center of charge is more distant from the substrate than OPT3 HOMO's center of charge displaced from the molecular center towards the thiol end.

To avoid misunderstandings, one should finally note that in this work the emphasis is on the fact that the asymmetric coupling of the dominant level to electrodes ($\Gamma_s \neq \Gamma_t$) does not give rise to current rectification in most real molecular junctions. This by no means implies that current rectification cannot be quantitatively described within the single level model. Along with the imbalance between the electrodes' (electro)chemical potential μ_x [Eq. (2)], an applied bias V may in general yield a (bias-driven) shift of the energy level

$$\varepsilon_0 \equiv \varepsilon_0|_{V=0} \xrightarrow{V\neq 0} \varepsilon_0(V) = \varepsilon_0 + \gamma_{\text{real}}\, eV. \tag{20}$$

This was quantitatively shown in experimental data analysis [45,46,61], with the important observation that the above γ_{real} turned out to be a parameter independent of Γ_s and Γ_t which is equal neither to γ entering Eq. (10c) nor to $\overline{\gamma}$ in Eq. (18b). It is the opposite energy shift direction caused by positive and negative biases that gives rise to rectification, which can be accounted for theoretically by means of the single model [cf. Eq. (1)],

$$\varepsilon_0(\ldots) \to \varepsilon_0(V),$$

wherein the V dependence is expressed by Eq. (20). In general, the dependence on V of $\varepsilon_0(V)$ expressed by Eq. (20) results from the interplay between intramolecular Stark effects [28] and the off-center spatial location of the MO's center of charge [19,62,63]. The latter (expression of the "lever" [19] or "potentiometer" [23,28] rule) results from convoluting the MO's spatial distribution with the local electric potential, whose determination requires simultaneously (self-consistently) solving the quantum mechanical (Schrödinger) and electrostatic (Poisson) equations. Such microscopic calculations turned out to be successful in quantitatively reproducing the RR of OPT3 junctions even subject to a mechanical deformation [64]. State-of-the-art *ab initio* calculations [23,28] showed that in alkanethiols the intramolecular Stark effect yields a strictly linear V dependence well beyond the bias range sampled in experiments [28,46].

To be on the safe side, we wrote above that $\Gamma_s \neq \Gamma_t$ cannot yield RR values significantly different from unity "in most real molecular junctions." The results deduced in this work showed that this is indeed the case irrespective of whether the charge transport is off-resonant [cf. Eq. (16)] or on-resonant. In situations escaping the model of Eq. (1)—unlikely in real molecules but still possible in artificial nanostructures where

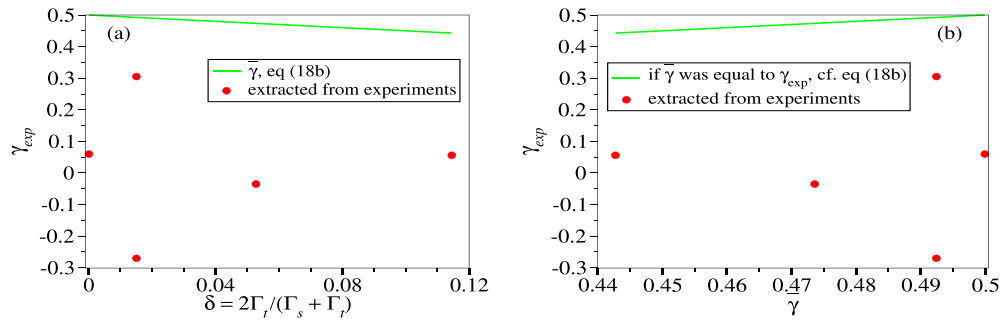

FIG. 4. (a) The bias-driven MO shift $\gamma_{\text{real}} \equiv \gamma_{\text{exp}}$ deduced from transport measurements plotted against the MO coupling asymmetry parameter δ defined by Eq. (18b) reveals that the latter parameter has no impact on current rectification. (b) If Eq. (18) was correct, $\overline{\gamma}$ and γ_{real} would be equal, but, as shown, they are not. Numerical values underlying this figure are collected in Table I.

electronic properties can be continuously tuned—close to resonance, the level's occupancy may be significantly different from 0 and V dependent [21–23,57]. If, furthermore, on-site electron-electron interactions [25,27] or electron-electron interactions at contacts [20] are strong, $\Gamma_s \neq \Gamma_t$ may lead to a certain I-V asymmetry, although spectacular RR values can hardly be expected on this basis. Problems arise in these cases because, close to resonance, electron couplings both to slow vibrational degrees of freedom (reorganization effects) and to fast phonons (deserving quantum-mechanical treatment) need to be considered.

V. CONCLUSION

It was not our aim here to explain current rectification in real molecular junctions using schematic (tight-binding, Hubbard, etc.) models extended, e.g., to also include interactions due to charge accumulation at interfaces considered in Sec. IV C. Realistic microscopic calculations showed that RR can be quantitatively described in real molecular junctions even subject to mechanical stretching [64] or in situations where, counterintuitively, the dominant MO does not track the substrate in its close proximity but rather the much more distant tip electrode [23,28].

Rather, in this work, we have presented analytic results deduced theoretically by exactly solving the nonequilibrium problem for a general quantum mechanical Hamiltonian describing the charge transport dominated by a single energy level. Technically speaking, the present study goes beyond the existing approaches to charge transport and related current rectification within a single dominant channel because we worked out the general equation Eq. (11) for the current by employing exact expressions for the embedding self-energies having (i) nonvanishing real parts [cf. Eq. (8b)] and (ii) imaginary parts that do depend on the energy [cf. Eq. (8a)].

The formulas deduced in this way enabled us to obtain numerical estimates based on parameter values extracted from transport measurements on benchmark junctions or even chosen to simulate rectification enhancement. On this basis, we can definitely rule out that unequal MO couplings to electrodes ($\Gamma_s \neq \Gamma_t$) make a significant contribution to current rectification in experiments with molecular junctions fabricated so far. This conclusion clearly contradicts some opposite claims in previous literature while confirming other assertions based on intuitive considerations [44,48].

Hypothetically, $\Gamma_s \neq \Gamma_t$ could yield (not large but still presumably) observable I-V asymmetry in the case of electrodes possessing extremely narrow conduction bands [low $W_{s,t}$ imply large γ; cf. Eq. (10c)]. Artificial nanostructures may be better suited for this purpose because their properties can be tuned more easily than those of real molecules. Still, in these cases electron correlations will certainly be very strong and will invalidate (Laudauer's) uncorrelated transport description underlying the vast majority of theoretical studies including the present one.

ACKNOWLEDGMENTS

The author gratefully acknowledges financial support from the German Research Foundation (DFG Grant No. BA 1799/3-2) in the initial stage of this work and computational support by the state of Baden-Württemberg through bwHPC and the German Research Foundation through Grant No. INST 40/575-1 FUGG (bwUniCluster 2, bwForCluster/MLS&WISO, and JUSTUS 2 cluster).

[1] A. Aviram and M. A. Ratner, Chem. Phys. Lett. **29**, 277 (1974).
[2] S. N. Yaliraki and M. A. Ratner, J. Chem. Phys. **109**, 5036 (1998).
[3] R. Metzger, Acc. Chem. Res. **32**, 950 (1999).
[4] A. Nitzan, Annu. Rev. Phys. Chem. **52**, 681 (2001).
[5] I. Diez-Peres, J. Hihath, Y. Lee, L. Yu, L. Adamska, M. A. Kozhushner, I. I. Oleynik, and N. Tao, Nat. Chem. **1**, 635 (2009).
[6] C. A. Nijhuis, W. F. Reus, and G. M. Whitesides, J. Am. Chem. Soc. **132**, 18386 (2010).
[7] P. Parida, S. K. Pati, and A. Painelli, Phys. Rev. B **83**, 165404 (2011).
[8] C. Jia and X. Guo, Chem. Soc. Rev. **42**, 5642 (2013).
[9] L. D. Wickramasinghe, M. M. Perera, L. Li, G. Mao, Z. Zhou, and C. N. Verani, Angew. Chem. Int. Ed. **52**, 13346 (2013).
[10] H. J. Yoon, K. C. Liao, M. R. Lockett, S. W. Kwok, M. Baghbanzadeh, and G. M. Whitesides, J. Am. Chem. Soc. **136**, 17155 (2014).
[11] R. M. Metzger, Chem. Rev. **115**, 5056 (2015).
[12] C. Van Dyck and M. A. Ratner, Nano Lett. **15**, 1577 (2015).
[13] D. Xiang, X. Wang, C. Jia, T. Lee, and X. Guo, Chem. Rev. **116**, 4318 (2016).
[14] J. Trasobares, D. Vuillaume, D. Théron, and N. Clément, Nat. Commun. **7**, 12850 (2016).
[15] X. Chen, M. Roemer, L. Yuan, W. Du, D. Thompson, E. del Barco, and C. A. Nijhuis, Nat. Nanotechnol. **12**, 797 (2017).
[16] A. Z. Thong, M. S. P. Shaffer, and A. P. Horsfield, Sci. Rep. **8**, 9120 (2018).
[17] R. Metzger, Nanoscale **10**, 10316 (2018).
[18] M. Baghbanzadeh, L. Belding, L. Yuan, J. Park, M. H. Al-Sayah, C. M. Bowers, and G. M. Whitesides, J. Am. Chem. Soc. **141**, 8969 (2019).
[19] I. R. Peterson, D. Vuillaume, and R. M. Metzger, J. Phys. Chem. A **105**, 4702 (2001).
[20] I. Bâldea, Chem. Phys. **400**, 65 (2012).
[21] I. Bâldea, Phys. Chem. Chem. Phys. **17**, 15756 (2015).
[22] I. Bâldea, Phys. Chem. Chem. Phys. **17**, 20217 (2015).
[23] I. Bâldea, Phys. Chem. Chem. Phys. **17**, 31260 (2015).
[24] G. Zhang, M. A. Ratner, and M. G. Reuter, J. Phys. Chem. C **119**, 6254 (2015).
[25] C. A. Stafford, Phys. Rev. Lett. **77**, 2770 (1996).
[26] I. Bâldea and H. Köppel, Phys. Rev. B **81**, 193401 (2010).
[27] M. Büttiker and D. Sánchez, Phys. Rev. Lett. **90**, 119701 (2003).
[28] Z. Xie, I. Bâldea, and C. D. Frisbie, Chem. Sci. **9**, 4456 (2018).
[29] T. N. Todorov, G. A. D. Briggs, and A. P. Sutton, J. Phys.: Condens. Matter **5**, 2389 (1993).
[30] T. N. Todorov, J. Phys.: Condens. Matter **14**, 3049 (2002).

[31] G. D. Mahan, *Many-Particle Physics*, 2nd ed. (Plenum Press, New York, 1990).
[32] C. Caroli, R. Combescot, P. Nozieres, and D. Saint-James, J. Phys. C: Solid State Phys. **4**, 916 (1971).
[33] A.-P. Jauho, N. S. Wingreen, and Y. Meir, Phys. Rev. B **50**, 5528 (1994).
[34] H. J. W. Haug and A.-P. Jauho, *Quantum Kinetics in Transport and Optics of Semiconductors*, 2nd rev. ed. Springer Series in Solid-State Sciences, Vol. 123 (Springer-Verlag, Berlin, 2008).
[35] Y. Xue, S. Datta, and M. A. Ratner, J. Chem. Phys. **115**, 4292 (2001).
[36] Y. Meir and N. S. Wingreen, Phys. Rev. Lett. **68**, 2512 (1992).
[37] S. Datta, *Quantum Transport: Atom to Transistor* (Cambridge University Press, Cambridge, UK, 2005).
[38] D. M. Newns, Phys. Rev. **178**, 1123 (1969).
[39] M.-C. Desjonqueres and D. Spanjaard, *Concepts in Surface Physics*, 2nd ed. (Springer-Verlag, Berlin, 1996).
[40] U. Peskin, J. Phys. B: At. Mol. Opt. Phys. **43**, 153001 (2010).
[41] W. Schmickler, J. Electroanal. Chem. **204**, 31 (1986).
[42] W. Schmickler, Chem. Phys. **289**, 349 (2003).
[43] M. G. Reuter, J. Chem. Phys. **133**, 034703 (2010).
[44] L. E. Hall, J. R. Reimers, N. S. Hush, and K. Silverbrook, J. Chem. Phys. **112**, 1510 (2000).
[45] Z. Xie, I. Bâldea, and C. D. Frisbie, J. Am. Chem. Soc. **141**, 3670 (2019).
[46] Z. Xie, I. Bâldea, and C. D. Frisbie, J. Am. Chem. Soc. **141**, 18182 (2019).
[47] I. Bâldea, Phys. Rev. B **85**, 035442 (2012).
[48] S. Datta, W. Tian, S. Hong, R. Reifenberger, J. I. Henderson, and C. P. Kubiak, Phys. Rev. Lett. **79**, 2530 (1997).
[49] Z. Xie, I. Bâldea, C. Smith, Y. Wu, and C. D. Frisbie, ACS Nano **9**, 8022 (2015).
[50] Q. V. Nguyen, Z. Xie, and C. D. Frisbie, J. Phys. Chem. C **125**, 4292 (2021).
[51] Z. Xie, I. Bâldea, A. T. Demissie, C. E. Smith, Y. Wu, G. Haugstad, and C. D. Frisbie, J. Am. Chem. Soc. **139**, 5696 (2017).
[52] I. Bâldea, Beilstein J. Nanotechnol. **7**, 418 (2016).
[53] J. C. Cuevas and E. Scheer, *Molecular Electronics: An Introduction to Theory and Experiment* (World Scientific, Singapore, 2010).
[54] G. Wang, Y. Kim, S.-I. Na, Y. H. Kahng, J. Ku, S. Park, Y. H. Jang, D.-Y. Kim, and T. Lee, J. Phys. Chem. C **115**, 17979 (2011).
[55] B. M. Briechle, Y. Kim, P. Ehrenreich, A. Erbe, D. Sysoiev, T. Huhn, U. Groth, and E. Scheer, Beilstein J. Nanotechnol. **3**, 798 (2012).
[56] L. Yuan, N. Nerngchamnong, L. Cao, H. Hamoudi, E. del Barco, M. Roemer, R. K. Sriramula, D. Thompson, and C. A. Nijhuis, Nat. Commun. **6**, 6324 (2015).
[57] I. Bâldea, Phys. Chem. Chem. Phys. **16**, 25942 (2014).
[58] I. Bâldea, J. Phys. Chem. C **117**, 25798 (2013).
[59] J. M. Artés, M. López-Martínez, A. Giraudet, I. Díez-Pérez, F. Sanz, and P. Gorostiza, J. Am. Chem. Soc. **134**, 20218 (2012).
[60] I. V. Pobelov, Z. Li, and T. Wandlowski, J. Am. Chem. Soc. **130**, 16045 (2008).
[61] C. E. Smith, Z. Xie, I. Bâldea, and C. D. Frisbie, Nanoscale **10**, 964 (2018).
[62] F. Zahid, M. Paulsson, and S. Datta, in Advanced Semiconductors and Organic Nano-Techniques, edited by H. Morkoç (Academic Press, San Diego, CA, 2003), Vol. 3, pp. 1–41.
[63] J. Zhang, A. M. Kuznetsov, I. G. Medvedev, Q. Chi, T. Albrecht, P. S. Jensen, and J. Ulstrup, Chem. Rev. **108**, 2737 (2008).
[64] Z. Xie, I. Bâldea, Q. Nguyen, and C. D. Frisbie, unpublished (2021); https://www.pci.uni-heidelberg.de/tc/usr/ioan/preprint_RR.pdf.